Bi *et al. Clinical Proteomics* (2025) 22:22
https://doi.org/10.1186/s12014-025-09544-6

Clinical Proteomics

RESEARCH Open Access

Multi-omics analyses, cell experiments, and network pharmacology tools identified key proteins and candidate drugs for alopecia areata treatment

Lingbo Bi[1,2†], Jing Wang[1†], Jungang Yang[1], Zhou Zhuang[1], Kejun Chen[1], Zining Xu[1], Xianbo Zuo[1], Jingkai Xu[1], Yujun Sheng[1*] and Yong Cui[1*]

Abstract

Purpose Alopecia Areata (AA) is an inflammatory non-cicatricial alopecia with a high prevalence. Some patients with AA show an inferior response to treatment. To find key proteins in AA, Genome-wide association study data from three cohorts were analyzed using Mendelian randomization (MR) method.

Patients and methods The gene expression of the identified proteins was further evaluated and compared between AA and healthy samples from two single-cell RNA datasets (GSE212447 and GSE233906). A cell model was also built to validate the findings. Autodock Vina and GROMACS, were also employed to search for ingredients from traditional Chinese medicine(TCM) that interacted with the identified protein.

Results Three proteins, DEFB1, HGFAC, and CYB5D2, were identified as potential drug targets. The altered gene expression in lesional samples of AA patients was consistent with the promoting or protective effects of identified proteins on the disease. The overexpression of risk factor DEFB1 upregulated the RNA and protein expression of MICA in HaCaT cells. The TCM ingredient cimigenol was found to interact with DEFB1 via molecular docking, and molecular dynamics simulations confirmed the stability of this interaction.

Conclusion DEFB1 is a potential drug target with promising prospects for the development of novel drugs for treating AA. The TCM ingredient, cimigenol, is a promising drug for AA treatment.

Keywords Inflammatory disorders, Mendelian randomization, Molecular Docking, Non-cicatricial areata, Single-cell transcriptome

†Lingbo Bi and Jing Wang contributed equally to this work.

*Correspondence:
Yujun Sheng
ahmusyj@163.com
Yong Cui
wuhucuiyong@vip.163.com
[1]Department of Dermatology, Friendship Hospital, Beijing 100029, China
[2]Graduate School, Peking Union Medical College, Chinese Academy of Medical Sciences, Beijing, China

Introduction

Alopecia Areata (AA) is a common inflammatory non-cicatricial alopecia that mostly manifests as a sudden occurrence of single or multiple plaque alopecia with a clear border [1]. In severe cases, the lesion can diffuse and eventually lead to hair loss in the entire scalp [2]. AA has a high recurrence rate and a long duration that can be up to several years or even decades in some patients [3]. Although AA is not life-threatening, patients still suffer from hair loss, anxiety, depression, and social stress [4].

Although various therapies have been developed, including glucocorticoids and small-molecule drugs, such as JAK inhibitors, some patients with AA show an inferior response to treatment [5]. Additionally, many patients report a high risk of relapse after cessation of drug use, making it important to discover new drug targets for AA [6]. Additionally, the financial burden of alopecia extends beyond treatment costs to encompass the social impact on the professional lives of patients, particularly those who are female, of Asian ethnicity, or have lower incomes [7, 8]. This underscores the urgent need to develop more affordable medication options for AA patients.

Previous studies have reported that circulating DNAs and cytokines may be causally associated with AA [9, 10]. However, the DNAs are too premature to directly intervene the biological process according to the central degoma and cytokines only represent a fraction of the bioactive factors. Meanwhile, the causal relationship between circulating proteins and AA has not yet been systematically investigated. As a technique for evaluating the causal association between exposure and outcome, Mendelian randomization (MR) has shown superior efficiency in identifying plasma proteins with promising potential as novel drug targets [11]. With abundant data from a large-scale genome-wide association study (GWAS), MR can predict the potential effects of drug targets on a disease and increase the chances of success in drug discovery.

In this study, we used MR to select the causal variation of AA with the potential to be a drug target by integrating and analyzing three independent GWAS summary datasets containing protein quantitative trait loci (pQTL) of plasma proteins. Phenome-wide MR (Phe-MR) was also performed to investigate possible side effects of the drug targets. The alteration of prioritized drug targets between lesional and non-lesional tissues was also evaluated and compared using two single-cell RNA (scRNA) datasets, GSE212447 and GSE233906. Furthermore, two network pharmacology tools, Autodock Vina and GROMACS, were employed to search and validate ingredients from traditional Chinese medicine (TCM) that interacted with drug targets.

Materials and methods

Acquiring instrument variables for proteins in plasma

Plasma pQTL data obtained from deCODE Genetics were used for exposure in the primary selection. Involving 35,559 Icelanders in GWAS, deCODE contained 4,907 plasma proteins and significant genetic associations (pQTLs). The selection of pQTLs in MR was based on the following criteria: first, the pQTL had a significant genetic association with a certain plasma protein ($p < 5e\text{-}08$) and was not located within the range of the major histocompatibility complex (MHC) region (chr6, 26–34 Mb); second, the pQTLs showed no linkage disequilibrium (LD) clumping ($r^2 < 0.1$, window size = 1000 Kb); and (should) a cis-acting pQTL (within 1 Mb range of gene for a lower pleiotropy).

Data from the UK Biobank Pharma Proteomics Project (UKB), which contained 54,219 participants and identified 2,923 proteins, were used for the validation of identified drug targets [12]. Additionally, proteome data from the Fenland Study with 4,775 proteins from 10,708 Caucasians were used for validation as well [13]. The selection of pQTLs in these two replication cohorts adhered to the same criteria outlined for the deCODE cohort.

GWAS summary statistics of AA

For both primary analysis and further validation, summary data obtained from the FinnGen database R11 were used as the outcomes. The GWAS summary data of the outcome were the AA dataset from the FinnGen R11 database (https://r11.finngen.fi/pheno/L12_ALOPECAREATA), which contained 862 patients with AA and 432,686 healthy participants.

MR analysis and study design for selection and validation of drug targets

MR analysis was developed to evaluate causal relationships without interference from confounding variables. In our study, the plasma proteins from the statistics in the deCODE, UKB, and Fenland studies were used as exposures, while AA was the outcome in the main MR analysis. The instrumental variables (IVs) were selected based on the criteria mentioned above. Using the "TwoSampleMR" package, the causal association between the protein with only one genetic instrument and AA was evaluated using the Wald ratio. The inverse variance weighted (IVW) method was used for other conditions. In addition, the MR Egger, Weighted median, simple mode, and weighted mode methods were used to evaluate the causal effects of proteins with more than two instruments. The increased risk of AA at the proteome level per standard deviation (SD) in blood is shown by the odds ratios (OR). The plasma proteins identified as being closely related to the risk of AA were prioritized as drug target candidates.

The causal effect of the drug target candidates on AA was further validated by MR analysis in the UKP and Fenland cohorts. Significance was also evaluated based on Bonferroni-corrected results [14]. We also employed the random effects model of the "metafor" package for the meta-analysis of the results in the three cohorts without heterogeneity and pleiotropy.

Phe-MR analysis investigated for side-effects of target proteins

To evaluate the potential side effects of the prioritized AA-associated proteins, Phe-MR analyses were performed on a range of diseases using the AstraZeneca PheWAS Portal (https://azphewas.com/) [15]. A significa nt risk or protection association will be determined with a p-value < 0.05/n in the Phe-MR analysis [16].

Sensitivity analysis

In the MR analysis, if a protein had more than two SNPs, the MR-Egger intercept test was employed to detect pleiotropy in the IVs of the exposure. Cochran's Q test was used to evaluate heterogeneity among IVs.

In addition, Bonferroni correction was employed in the MR analysis to lower the potential false discovery rate (FDR) after multiple tests. A threshold of $p < 0.05/n$ was used to determine whether the causal association was significant [17].

Analysis based on ScRNA expression dataset

Based on scRNA-seq data of biopsy samples from healthy controls and lesional areas with alopecia areata, the altered expression of genes encoding drug target proteins in specific cells was further evaluated. Gene expression profiles GSE212447 and GSE233609 were downloaded from the GEO database, and the original data were preprocessed and converted using the "Scanpy" package. After removing cells whose gene count was less than 200 and genes that were expressed in fewer than three cells in the sample, the RNA count was normalized and scaled with the "scanpy.pp.normalize_total" function. After data preprocessing, principal component analysis (PCA) and the "scanpy.tl.umap" functions were used to reduce the dimensionality of the merged dataset and visualize the expression of drug targets in different cell types. The "FindMarkers()" function and "clusterProfiler" package were employed in the gene set enrichment analysis(GSEA) to investigated the signaling pathways enriched in the keratinocytes of GSE212447.

Plasmid transfection

The plasmid was constructed (Corues Biotech, Nanjing, China), and cultured in RPMI 1640 medium supplemented with 10% FBS transfected with a plasmid carrying the DEFB1 fragment (DEFB1 sequences: ATGAGAA CTTCCTACCTTCTGCTGTTTACTCTCTGCTTACT TTTGTCTGAGATGGCCTCAGGTGGTAACTTTCTC ACAGGCCTTGGCCACAGATCTGATCATTACAATT GCGTCAGCAGTGGAGGGCAATGTCTCTATTCTGC CTGCCCGATCTTTACCAAAATTCAAGGCACCTGT TACAGAGGGAAGGCCAAGTGCTGCAAG) or empty plasmid in 12-well plates. The plasmid was transfected using CRTrans reagent (Abcam, USA).

Quantitative PCR

Total RNA was isolated from cultured cells using an RNA Isolation Kit (Vazyme, Nanjing, China), following the manufacturer's protocol. The extracted RNA was then reverse-transcribed into cDNA using HiScript III RT SuperMix for qPCR (Vazyme, Nanjing, China). ChamQ SYBR Color qPCR Master Mix (without ROX) (Vazyme, Nanjing, China) was employed in accordance with the specifications of the Bio–Rad CFXTM Real-Time PCR Detection System for quantitative PCR. Sequences of the DEFB1 primers used for real-time PCR were constructed by Corues Biotech.

Western blotting

In the cell experiment, fibroblasts were collected after transfection and lysed in RIPA buffer (Thermo Fisher Scientific) with protease inhibitors (Thermo Fisher Scientific). The acquired proteins were quantified, separated by sodium dodecyl sulfate-polyacrylamide gel electrophoresis, and electroblotted to PVDF membranes. After blocking for 1 h at room temperature, the PVDF membranes were incubated with primary antibodies overnight and then with HRP-conjugated secondary antibodies at 4 °C. The primary antibodies used were anti-β-actin (1:10000, Proteintech, 20536-1-AP), anti-GAPDH(1:10000, Proteintech, 60004-1-Ig), anti-DEFB1(1:1000, Proteintech, 14738-1-AP), anti-TGFβ1(1:5000, Proteintech, 81746-2-RR), anti-SMAD2 (1:2000, Proteintech, 12570-1-AP), anti-p-SMAD2(1:1000, Proteintech, 80427-2-RR), and anti-MICA (1:1000, Proteintech, 66384-1-Ig). The bands were visualized using HRP substrate on a ChemiDocTM XRS + system (Bio-Rad).

Targeted screening for drugs interacted with drug targets via molecular docking

To identify new options for AA treatment, we searched for drugs that interact with DEFB1 in the Traditional Chinese Medicine Systems Pharmacology Database and Analysis Platform (TCMSP) database via molecular docking [18]. Based on the proteomic structure of drug targets downloaded from Uniprot, AutodockVina 1.5.7 was employed to evaluate predicted binding energy (PBE) and interaction between the Chinese herbal medicinal ingredients and DEFB1. We obtained the molecular structures of the herbal medicinal ingredients from

TCMSP. The parameters for better druggability were set as follows: the blood-brain barrier (BBB) < −0.3, oral bioavailability (OB) > 30, and drug-likeness (dl) > 0.18 [19]. In addition, the molecular weight (MW) < 500 for a better drug absorption while the value of BBB should be less than − 0.3 to reduce possible neurotoxicity in the central nervous system. Discovery Studio Visualizer was employed to visualize the compound-protein interaction.

Molecular docking simulation

Before the molecular docking simulation, a system was prepared using a solution builder module. The systems were set into a cubic box and solvated using the TIP3P water model with antagonist sodium ions and hydrogen atoms to neutralize the charge. The edge of the box was at a minimum distance of 1 nm from the protein. The condition of the system was similar to that of the physiological environment, and the energy minimization step was performed using the Steepest Descent algorithm to eliminate any abnormal contacts between the protein and the surrounding water molecules.

After the system was equilibrated, the restraints on the protein were removed, and a 100 ns production molecular dynamics simulation was performed in GROMACS [20]. The production simulation was conducted under NPT conditions, maintaining a temperature of 300 K and pressure of 1.0 atm. The time step was set to 2 fs and all hydrogen-containing bond lengths were constrained using the SHAKE algorithm.

Cell viability test

The toxicity of selected drug was evaluated according to the viability of HaCaT cells with the Cell Counting Kit-8 (CCK-8). Briefly, the HaCaT cells were cultured with different concentrations of Cimigenol (MCE, HY-N6988) in a 96-well plate. After 24-hours culture, the CCK-8 reagent was added and the absorbance at 450 nm was measured 2 h later.

Results

Screening and validating proteins with causal effects on AA at the proteomic level

As is shown in Fig. 1, 1799 plasma proteins in the deCODE study had applicable IVs, among which the MR method revealed significant causal associations between 224 proteins and AA. After Bonferroni correction, the causal associations between the six plasma proteins and AA, including DEFB1, MRC1, HGFAC, BRD2, ADGRE2, and CYB5D2, remained significant ($p < 0.05/1799$) (Supplementary Table S1). Sensitivity analysis was conducted to investigate the potential heterogeneity and pleiotropy in these causal associations. Cochran's Q test and the MR-Egger intercept test detected no heterogeneity and pleiotropy in the causal association.

To validate their potential as novel drug targets for AA, the six drug target candidates whose causal effects remained significant after the Bonferroni correction were searched in two other independent cohorts for replication (Fenland study and UKBPPP study).

Under the same stringent criteria employed in the deCODE analysis, we identified four proteins with closely related pQTLs (IVs) in the Fenland study. The significant causal effects of three proteins, including DEFB1 (OR = 1.478, 95%CI = 1.240–1.761, p = 1.27E-05), HGFAC (OR = 0.881, 95%CI = 0.828–0.937, p = 5.97E-05), and CYB5D2 (OR = 0.754, 95%CI = 0.618–0.919, p = 5.250E-03), were confirmed on AA after the Bonferroni correction ($p < 0.05/4$). These results were consistent with those found in the discovery cohort. BRD2, however, was not validated in the Fenland cohort. Sensitivity analysis excluded the presence of both heterogeneity and pleiotropy in all three proteins.

Among the six candidate drug targets identified in the deCODE cohort, only two, MRC1 and ADGRE2, had applicable IVs in the UKBPPP study. However, none of these three proteins were causally associated with AA based on the results of the MR analysis.

A meta-analysis was also conducted for proteins with more than one heterogeneity- and pleiotropy-free result across the three independent cohorts. Candidate proteins, including DEFB1, HGFAC, CYB5D2, and ADGRE2, were supported by meta-analysis as drug targets for AA.

Three proteins with validated causal effects were identified as promising drug targets for AA treatment, including DEFB1, HGFAC, and CYB5D2 (Fig. 2A).

Phe-MR analysis on target proteins for potential side effects

Phe-MR analysis was conducted to assess the potentially beneficial or deleterious effects of the five identified drug targets on other traits. Based on the data covering 17,361 dichotomous phenotypes and 1,419 quantitative phenotypes in the AstraZeneca PheWAS Portal database, the related traits of these drug targets for AA were investigated. Only DEFB1 was causally related to a higher risk of sepsis due to the Streptococcus group (Fig. 2B). No other proteins were found to be significantly related to the traits in the PheWAS Portal (Fig. 2C and D). Detailed information on potential side effects is presented in Supplementary Table S2.

Cell-specific expression analysis

The expression of genes that encode the drug-target proteins was further evaluated in specific cells based on two single-cell RNA-seq datasets from biopsy samples of AA patients, including GSE212447 and GSE233906. The expression profile of GSE212447, which contained 28,851 genes in 43,671 cells, was downloaded from the GEO

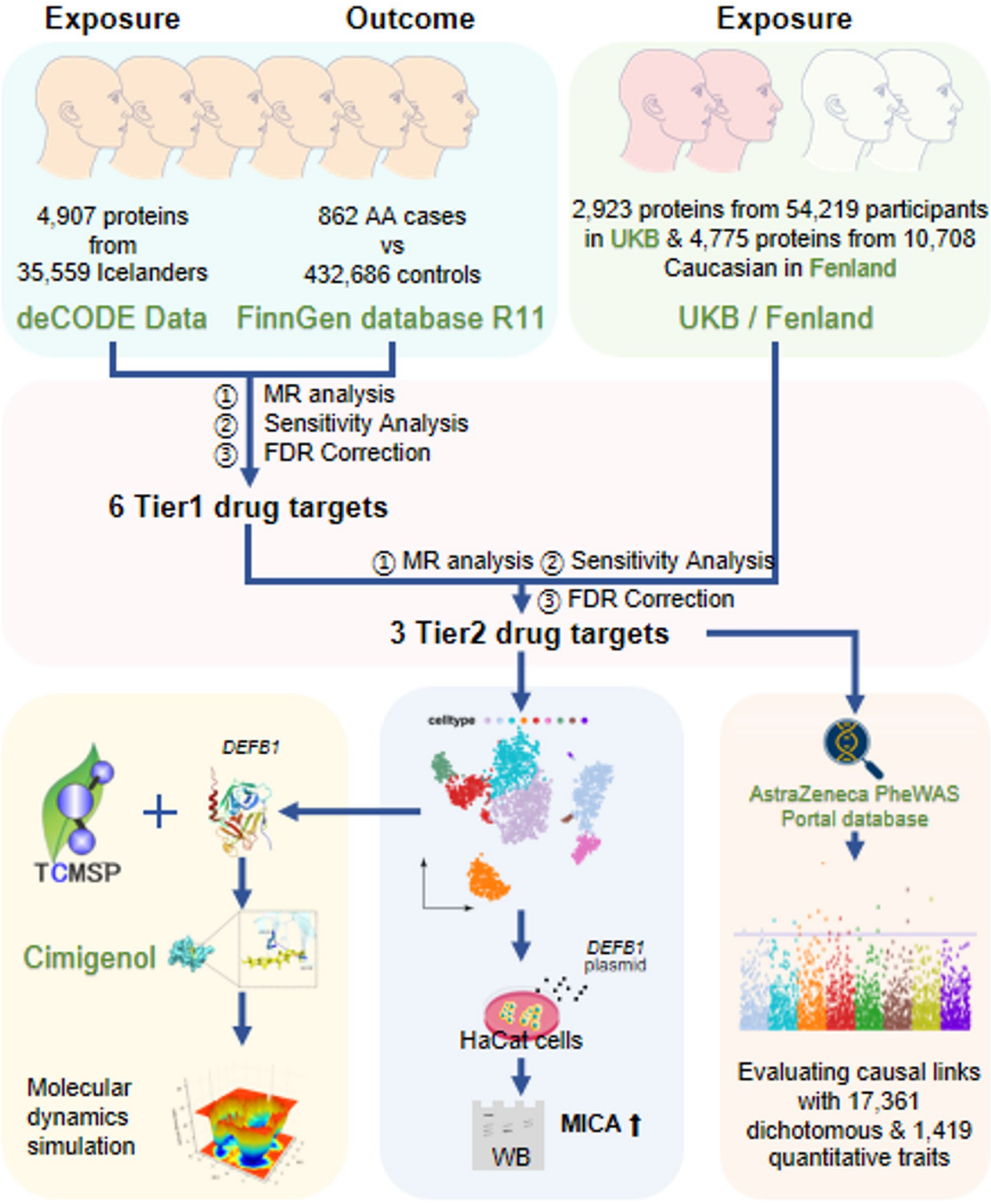

Fig. 1 The flow chart displays the overall design of the study. The details of drug targets selection and validation as well as the following investigation were contained in this figure

A

gene	deCODE		UKB		Fenland		Meta	
	OR (95% CI)	P value	OR (95% CI)	P value	OR (95% CI)	P value	OR (95% CI)	P value
DEFB1	1.43 (1.26 − 1.64)	8.63e−08			1.48 (1.24 − 1.76)	1.27e−05	1.45 (1.30 − 1.61)	5.11e−12
MRC1	1.21 (1.11 − 1.30)	2.60e−06	0.87 (0.66 − 1.15)	3.38e−01			1.05 (0.77 − 1.44)	7.35e−01
HGFAC	0.87 (0.82 − 0.93)	1.05e−05			0.88 (0.83 − 0.94)	5.97e−05	0.88 (0.84 − 0.91)	2.61e−09
BRD2	0.01 (0.00 − 0.09)	1.24e−05						
ADGRE2	0.75 (0.65 − 0.85)	1.44e−05	0.86 (0.72 − 1.02)	8.74e−02	0.86 (0.71 − 1.05)	1.37e−01	0.81 (0.73 − 0.89)	2.34e−05
CYB5D2	0.60 (0.48 − 0.76)	1.50e−05			0.75 (0.62 − 0.92)	5.25e−03	0.68 (0.55 − 0.85)	5.37e−04

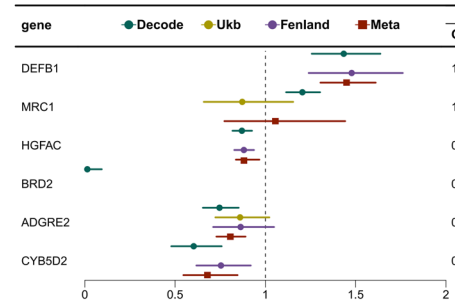

B

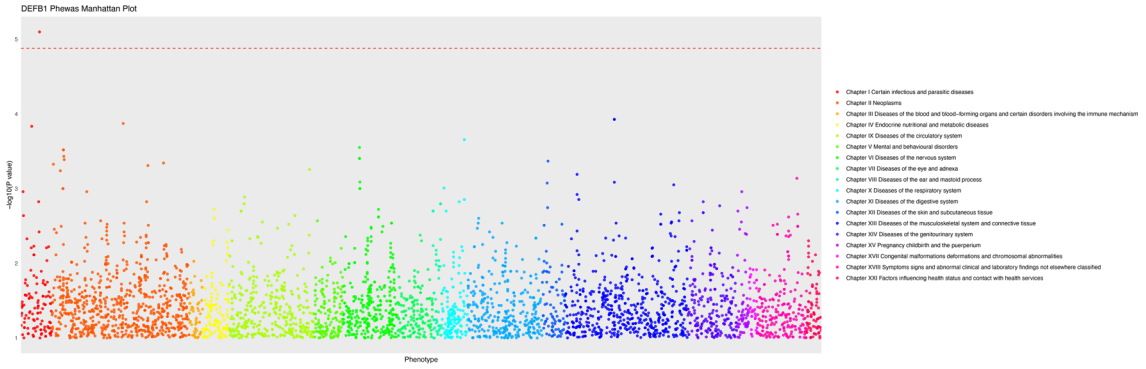

C

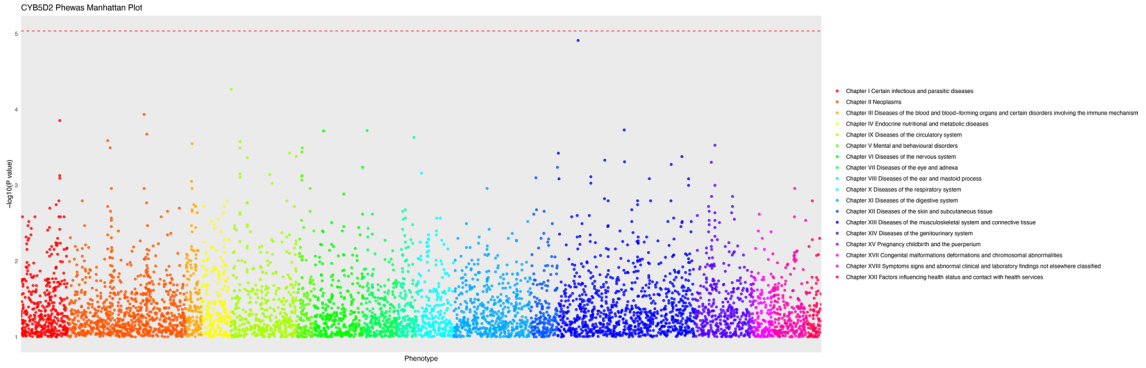

D

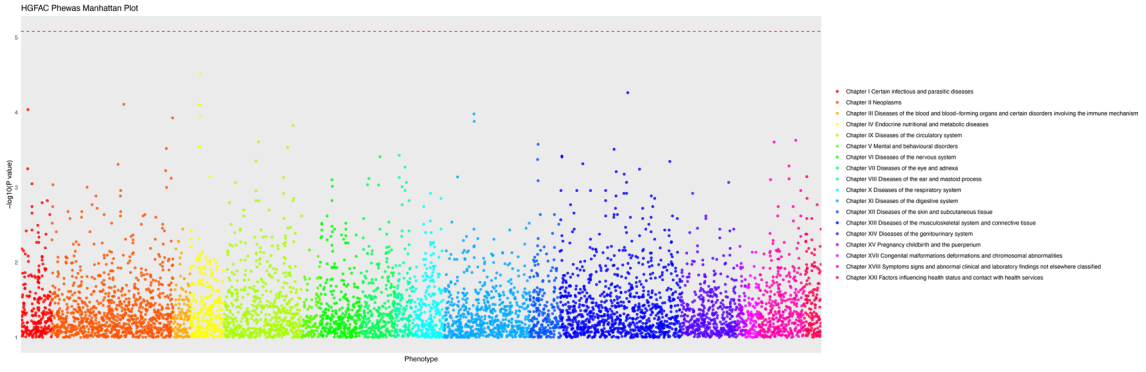

Fig. 2 The figure contains the results of MR and Phe-MR analysis. The significance of causal association between 6 candidates of drug target and AA is evaluated by MR analysis on three independent cohorts (**A**). The results of the meta-analysis based on the statistics from MR are also shown in this forest plot (**A**). The dot plots illustrate the causal effects of identified drug targets, including DEFB1 (**B**), CYD5B2 (**C**), and HGFAC (**D**), on both dichotomous and quantitative phenotypes in the AstraZeneca database. The red dotted line represents the threshold for Bonferroni-corrected p-values

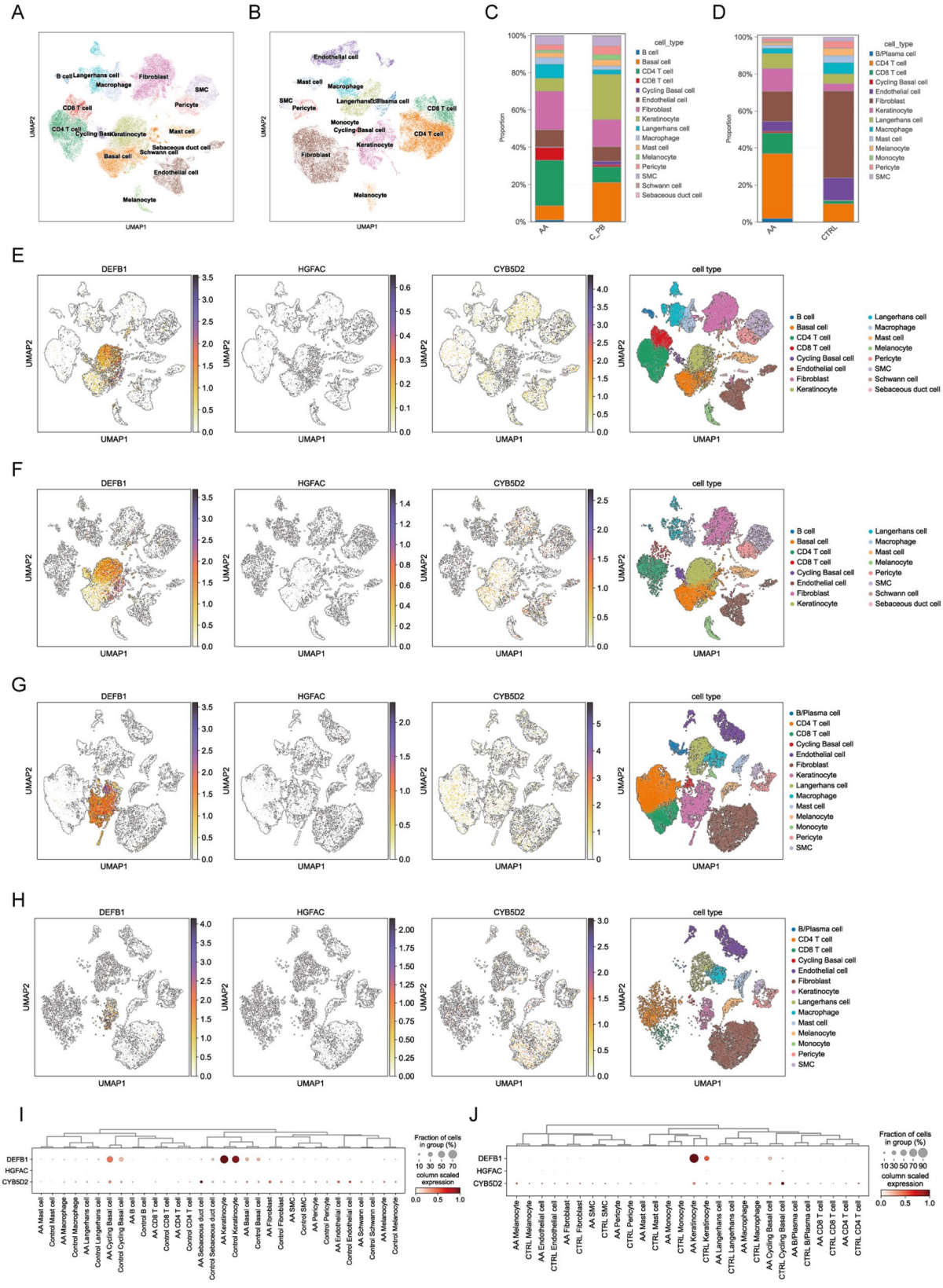

Fig. 3 (See legend on next page.)

(See figure on previous page.)

Fig. 3 The figure displays the altered expression of identified drug targets in the two scRNA datasets. The identified cell types of GSE212447 (**A**) and GSE233906 (**B**) are shown. The alteration of cell proportion between AA and control group is also displayed (**C**: GSE212447 and **D**: GSE233906). The umap plots visualize the changes in cell-specific expression of identified drug targets between AA and control groups in GSE212447 (**E** and **F**) and GSE233906 (**G** and **H**). The dot plots visualize the changes in the proportion of each cell type that expressed drug target genes as well as the cell-specific expression level between AA and control groups in GSE212447 (**I**) and GSE233906 (**J**)

database. Samples from GSM6532919 to GSM6532922 were defined as the diseased group ($n = 4$), whereas samples from GSM6532923 to GSM6532925 were defined as the control group ($n = 3$).

In GSE233906, only eight human samples were included in the analysis, including 30,228 genes in 36,899 cells. Two patients (GSM7438946 and GSM7438947) and six patients (GSM7438941 to GSM7438945 and GSM7438948) were defined as the control group and the diseased group, respectively.

The cell clusters in the two datasets are shown in Fig. 3. The cells were divided into 16 cell types (Fig. 3A) in GSE212447 and 14 cell types in GSE233906 (Fig. 3B). Compared with the control groups, the proportion of immune cells in the AA group increased in both datasets(Fig. 3C and D). The expression of DEFB1 was sightly upregulated in the keratinocytes of AA patients in the GSE212447 dataset (Fig. 3E and F). A similar trend was observed in GSE233906 but was significantly more pronounced (Fig. 3G and H). DEFB1 expression in cycling basal cells and the proportion of cells that expressed DEFB1 increased in patients with AA (Fig. 3I and J). However, the proportion of cells that expressed HGFAC and CYB5D2 was relatively low in both the datasets (Fig. 3I and J).

Transfection efficiency of DEFB1

The mRNA level of DEFB1 was significantly elevated in HaCaT cells 24 h and 48 h after DEFB1 overexpression (Fig. 4A). Transfection efficiency peaked at 48 h. Meanwhile, the protein expression of DEFB1 also increased the most at 48 h after overexpression ($p < 0.05$, Fig. 4B). The following experiments were conducted using HaCaT cells after 48 h of transfection.

DEFB1 overexpression promotes the expression of MICA in HaCaT cells by activating TGFβ/SMAD2 pathway

To explore the effect of DEFB1 overexpression in AA, we further evaluated MICA expression in DEFB1 overexpressed HaCaT cells. The qPCR revealed that overexpression of DEFB1 upregulated the RNA expression of MICA in HaCaT cells (Fig. 5A). The protein levels of MICA were also significantly increased in HaCaT cells after transfection with DEFB1(Fig. 5B).

Additionally, the GSEA revealed that the TGFβ/SMAD signaling pathway was enriched in the keratinocytes of GSE212447 (Fig. 5C and D). Therefore, we validated this finding in the HaCaT cells and found that the TGFβ/SMAD2 pathway was activated by the DEFB1 overexpression(Fig. 5E).

Prediction of compounds interacted with identified drug targets

Based on the above results, DEFB1, a risk factor for AA, was selected as the target for drug selection via molecular docking. We firstly ran the selection on 13,144 TCM ingredients based on the parameters mentioned above (Fig. 6A). Then we prioritized potential of the remained TCM ingredients to inhibit DEFB1, with a focus on their binding affinity (Fig. 6B). As a result, 545 TCM ingredients that met the standards were found to be applicable for inhibiting DEFB1, with the lowest PBE under -9 kcal/mol. Cimigenol had the lowest PBE (-9.8 kcal/mol). The binding positions and interactions between the candidate ingredients and DEFB1 were obtained and visualized (Fig. 6C and D).

Molecular dynamics simulations

After approximately 50 ns of reaction, complexes were formed stably, according to the root-mean-square deviation (RMSD) and solvent-accessible surface (Fig. 7A and B). The radius of gyration curve remained stable throughout most of the binding process, except for minor fluctuations before 50 ns (Fig. 7C). According to the root-mean-square fluctuation (RMSF) plot, residues near the predicted binding site (including residues 15, 20, and 29) in DEFB1 have outstanding flexibility when bound to cimigenol (Fig. 7D). The 2D (Fig. 7E) and 3D (Supplementary Figure S1) plots of the free-energy landscape (FEL) depict the distribution of free energy across different conformations of the system. Blue dots represent energetically favorable conformations, whereas red dots represent unfavorable conformations. According to the FEL plot, the DEFB1-Cimigenol complex can adopt a stable conformation characterized by a very low Gibbs energy, which is represented by the lowest points on the bottom of the 3D plot (Supplementary Figure S1).

The assessment of the binding stability between a ligand and a receptor is based on the binding free energy calculated using the Molecular Mechanics/Poisson-Boltzmann Surface Area (MM/PBSA) method. The overall predicted interaction energy between Cimigenol and DEFB1 was -13.04 kcal/mol (Fig. 7F). The GGAS and GSOLV were -16.80 and 3.76 kcal/mol, respectively.

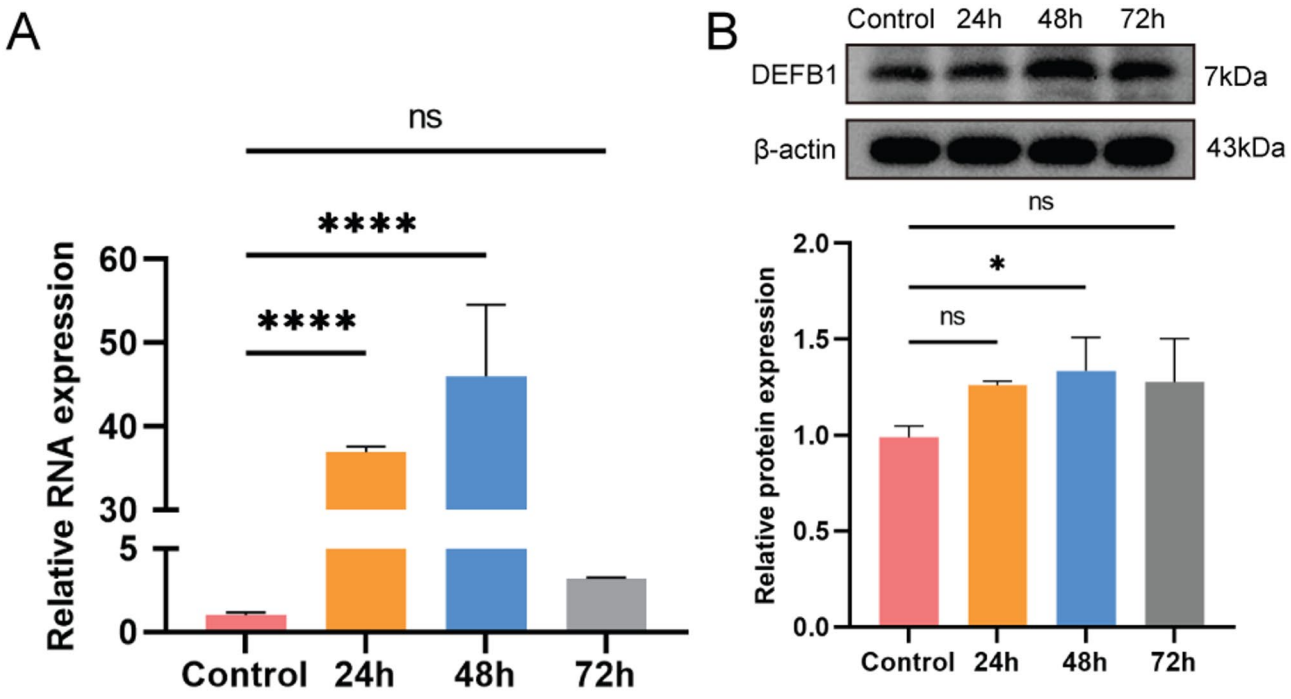

Fig. 4 The figure shows the DEFB1 transfection efficiency in HaCaT cells at different timepoints after the transfection. The RNA (**A**) and protein (**B**) expression of DEFB1 both evaluated significantly after 48 h transfection with plasmid

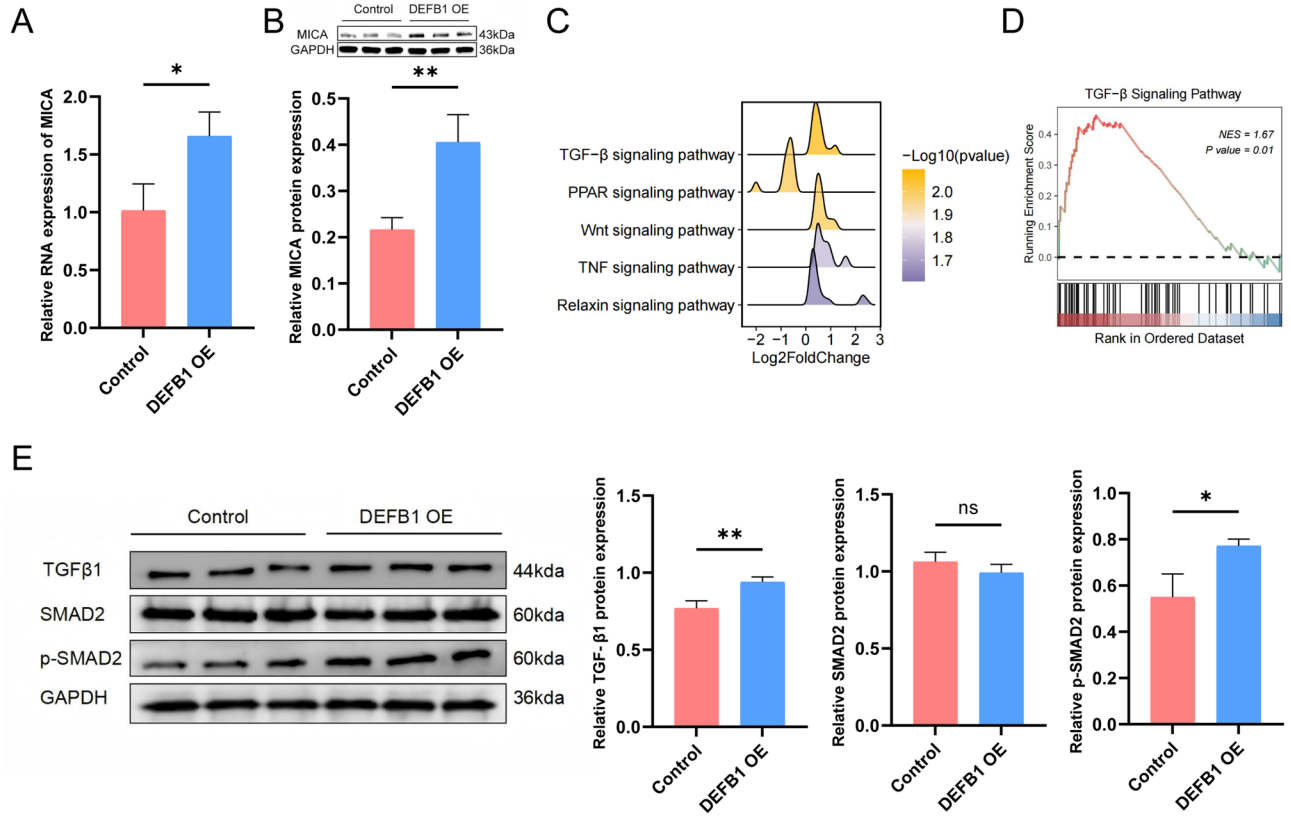

Fig. 5 The alteration of MICA expression and TGFβ/SMAD pathway after the DEFB1 overexpression. The RNA (**A**) and protein expression (**B**) of MICA both increased in HaCaT cells after the DEFB1 overexpression. The TGFβ/SMAD pathway was enriched in the AA samples of GSE212447 (**C** and **D**). The same pathway activation was also detected after the DEFB1 overexpression (**E**)

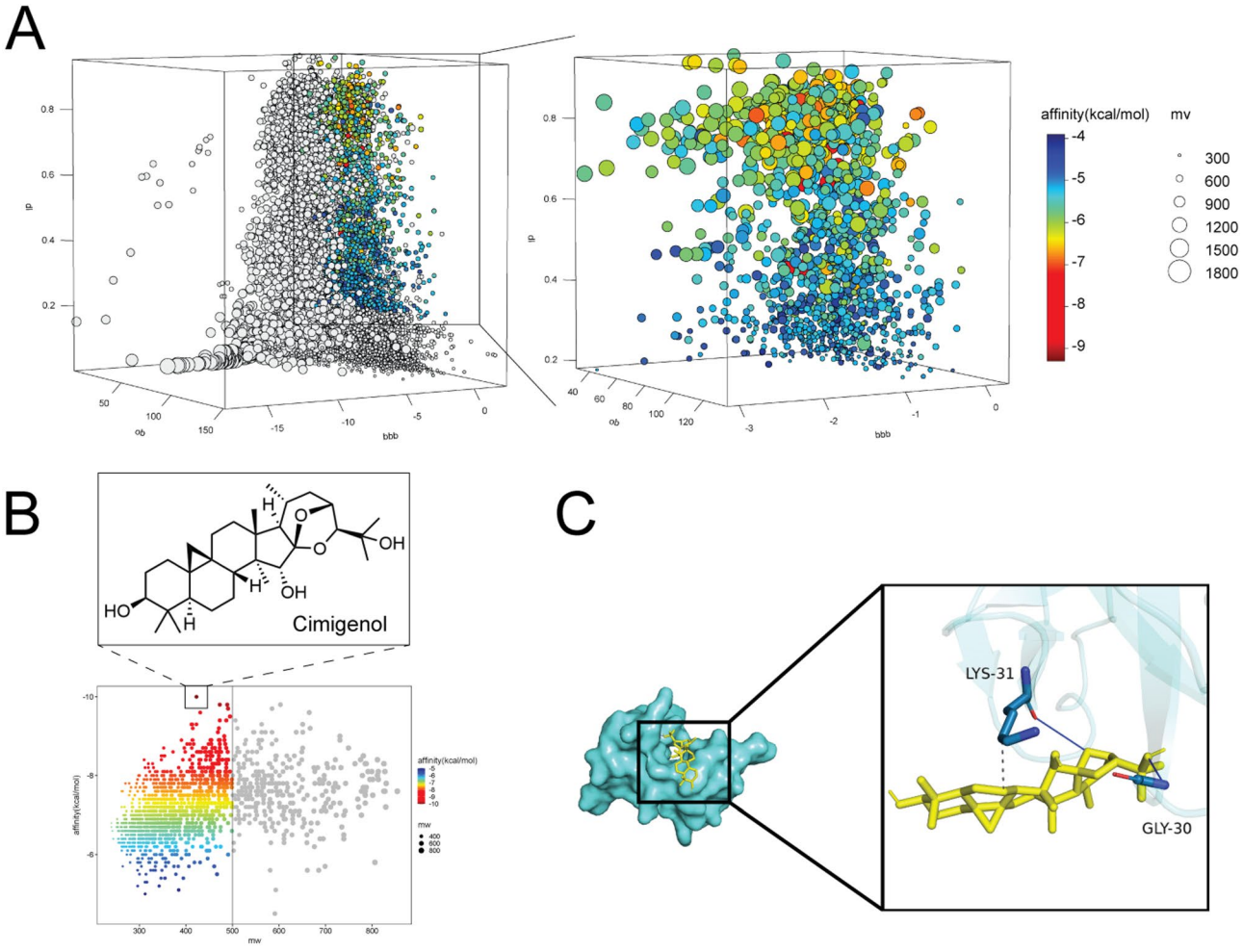

D

Hydrophobic Interactions

Index	Residue	AA	Distance	Ligand Atom	Protein Atom
1	31B	LYS	3.84	613	566

Hydrogen Bonds

Index	Residue	AA	Distance H-A	Distance D-A	Donor Angle	Protein donor?	Side chain	Donor Atom	Acceptor Atom
1	30A	GLY	2.73	3.06	100.23	✓	×	243 [Nam]	638 [O3]
2	31B	LYS	3.36	3.73	104.93	×	×	627 [O3]	563 [O2]

Fig. 6 (See legend on next page.)

(See figure on previous page.)

Fig. 6 The plot depicts the process of virtual selection. The TCM ingredients in TCMSP were filtrated based on their OB, dl, and, BBB. The remained TCM ingredients with MW under 500 were prioritized according their affinity with DEFB1. The visualized 3D graph picture shows the protein (the green structure) wrapping the Cimigenol particle (the yellow structure) (**C**). Residues Gly-30 A bind the Cimigenol through the hydrogen bonds (blue line) while the Lys-31B binds the Cimigenol through both hydrogen bonds and hydrophobic interactions (grey dotted line). The table contained detailed information of the interacting bonds between Cimigenol and DEFB1(**D**)

Cimigenol reversed the increased MICA expression and TGFβ/SMAD2 pathway activation in vitro

We firstly investigated the toxicity of Cimigenol in vitro and chose the 1μM as the Cimigenol concentration in the following experiments (Fig. 8A). We found that the Cimigenol treatment inhibited the increased protein level of DEFB1 after the transfection (Fig. 8B). Furthermore, the activation of TGFβ/SMAD2 pathway and elevated expression of MICA were also reversed after the Cimigenol combined with the DEFB1 protein.

Discussion

AA patients are reported to have abnormal levels of certain kinds of circulating blood components such as DNAs, antibodies, and cytokines [10, 21]. The treatment targeting these components showed satisfying treatment efficacy [22]. The level of plasma components such as IL-4 can be promising biomarkers in predicting the prognosis [23]. This evidence inspired us to comprehensively investigate the causal effect of circulating proteins on psoriasis and provides evidence supporting the potential of plasma proteins as therapeutic targets. By employing MR analysis, plasma proteins from three independent large-scale cohorts were evaluated for their potential in treating AA, which is the first study to report a causal association between plasma proteins and AA. Three plasma proteins, including one risk factor (DEFB1) and two protective factors (HGFAC and CYB5D2), were prioritized as drug targets with high potential for AA treatment.

The risk factor DEFB1, also known as HBD-1, is an antimicrobial peptide that is widely expressed in epithelial cells of humans [24, 25]. The plasma levels of DEFB1 are associated with multiple autoimmune diseases that present with cutaneous symptoms [26, 27]. Several pathways activated by DEFB1, including chemotaxis, apoptosis, and neutrophil extracellular traps (NETs), may contribute to this process [28]. The DEFB1 in circulation was found to correlate with IFN-γ, a key inducer of inflammation in AA [29]. The increased expression of DEFB1 caused by IFN-γ was also observed in keratinocytes, which can be reversed by the inhibition of JAK2, indicating the participation of the JAK/STAT signaling pathways [30]. The pivotal role of the JAK/STAT signaling pathway has been strengthened in the pathogenesis of AA, suggesting that DEFB1 is a potential effector of IFN-γ-induced JAK/STAT activation in AA [31]. There is also evidence supporting that the overexpression of DEFB1 increases STAT3 phosphorylation and total STAT3 [32]. Such a positive feedback loop may amplify the level of phosphorylated STAT3 and lead to an autoimmune response that targets the hair follicles. Furthermore, as a first-line therapy for AA, corticosteroids inhibit the expression of DEFB3, but not DEFB1 and 2, which may explain why some AA patients react poorly to local injection or oral dosage of corticosteroids [33, 34].

In cellular experiments, we discovered compelling evidence suggesting that DEFB1 plays a potential role in the pathogenesis of AA. Keratinocytes overexpressing DEFB1 exhibited elevated levels of MICA both at the RNA and protein levels. MICA has long been considered a trigger for the loss of immune privilege, contributing to the autoimmune response targeting hair follicles [35]. A previous study showed that the increased MICA expression in HF keratinocytes induced by the oxidative stress may activate the receptor NKG2D of NK cells and CD8 + T cytotoxic cells, leading to destabilization of the HF immune-privileged site [36]. Our findings suggest that inhibition of DEFB1 could be a promising therapeutic approach for treating AA.

To further explore suitable TCM ingredients that can be used as DEFB1 inhibitors, we employed AutoDock to prioritize the TCM ingredient that binds to DEFB1 with the lowest binding energy and identify the specific binding site on the protein. The RMSF plot revealed the flexibility of the residues near the identified binding site, suggesting the possible existence of pocket-like structures in DEFB1 upon binding to the drug. The binding process that was later simulated by GROMACS was stable, indicating the potential of cimigenol in inhibiting DEFB1. Furthermore, the criteria used in drug screening include the requirements for MW, DL, and BBB permeability to ensure better druggability and safety. According to previous studies, cimigenol is a novel cycloartane triterpenoid extracted from *Cimicifuga* that has been reported to have immunomodulatory and anti-inflammatory effects [37, 38]. After the virtual selection and molecular dynamic simulation, we further revealed that Cimigenol reversed the pathway activation and MICA expression induced by DEFB1, suggesting its potential to be a novel option for the AA treatment. Our study is the first to report the possible inhibitory effect of Cimigenol on DEFB1 using network pharmacologic tools. However, the precise interaction between Cimigenol and DEFB1 requires further investigation, both in vitro and in vivo.

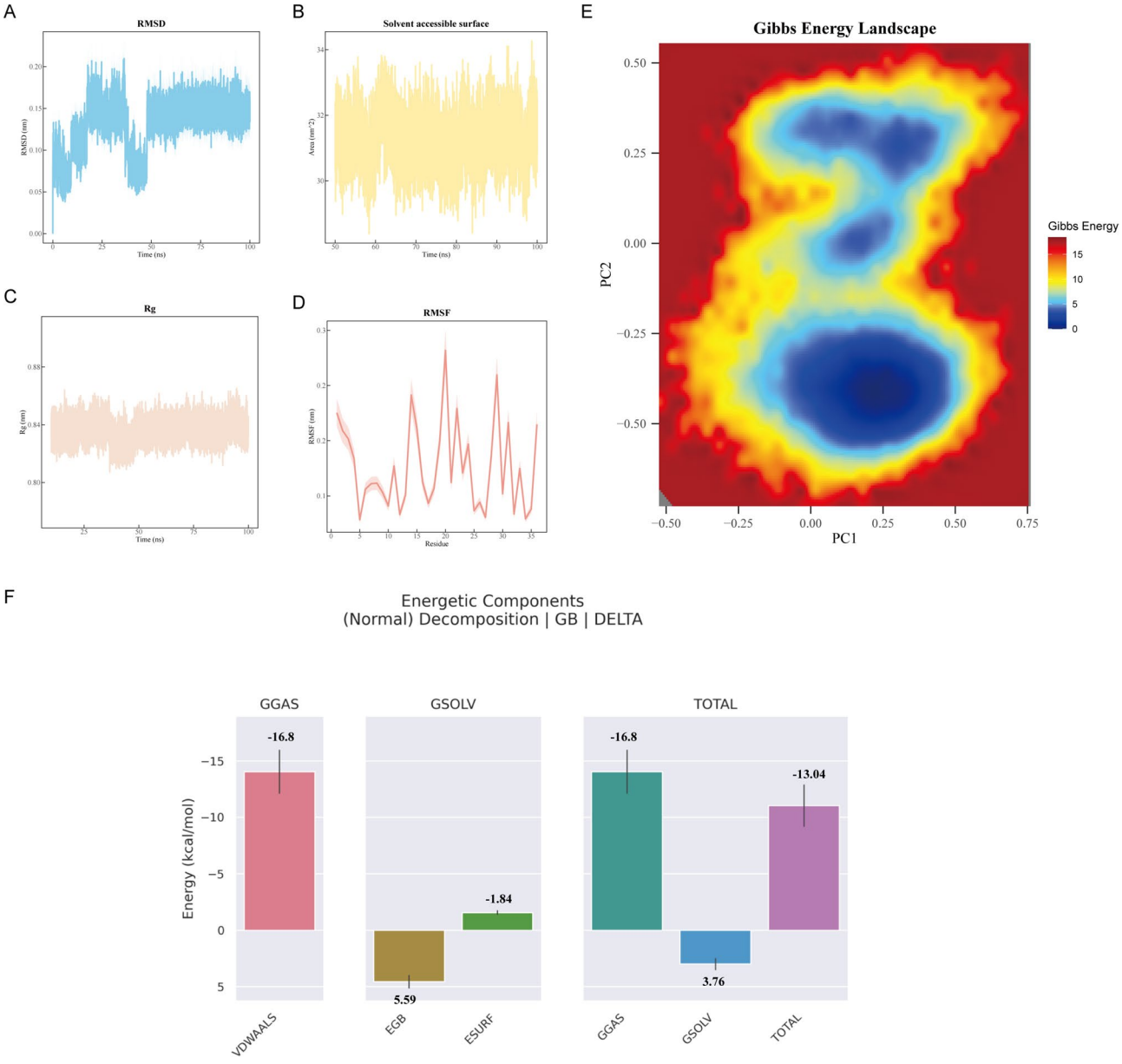

Fig. 7 The plot illustrates the details of molecular dynamics simulations conducted using AutoDock and GROMACS. The RMSD (**A**), SASA (**B**), and radius of gyration (**C**) plots indicate a stable conformation following protein-drug binding, with only minor fluctuations observed before 50 ns. The RMSF plot highlights the residues exhibiting significant flexibility upon binding with Cimigenol (**D**). The 2D Free Energy Landscape (FEL) plot depicts the distribution of free energy across different system conformations (**E**). The predicted energy of drug-protein binding indicates a stable complex (**F**)

HGFAC, a coagulation factor XII-like serine endopeptidase, mostly exists in circulation as a zymogen (proHGFAC) and stimulates the transformation of proHGF to HGF, inducing repair in injured tissues. HGF has been reported to promote angiogenesis in the hair follicles [39]. On the scalp, local HGF can promote the growth and pigmentation of human hair by activating the Wnt/β-catenin pathway [40]. Therefore, HGFAC, although not detected in scalp samples in the scRNA datasets, may promote hair regrowth and suppress inflammation in AA by inducing the production of HGF [41].

CYB5D2, also known as ferricin, belongs to the membrane-associated progesterone receptor (MAPR) family. CYB5D2 is a novel extracellular heme-binding protein that promotes neurogenesis [42]. In HeLa cells, CYB5D2 showed protective effects against etoposide-induced cytotoxicity and enhanced cell survival [43]. In this study, we detected decreased expression of CYB5D2 in cycling basal cells of AA samples, the division and proliferation of which are critical for tissue repair [44]. The reduced proliferation induced by decreased CYB5D2 expression may increase the vulnerability of the hair follicles.

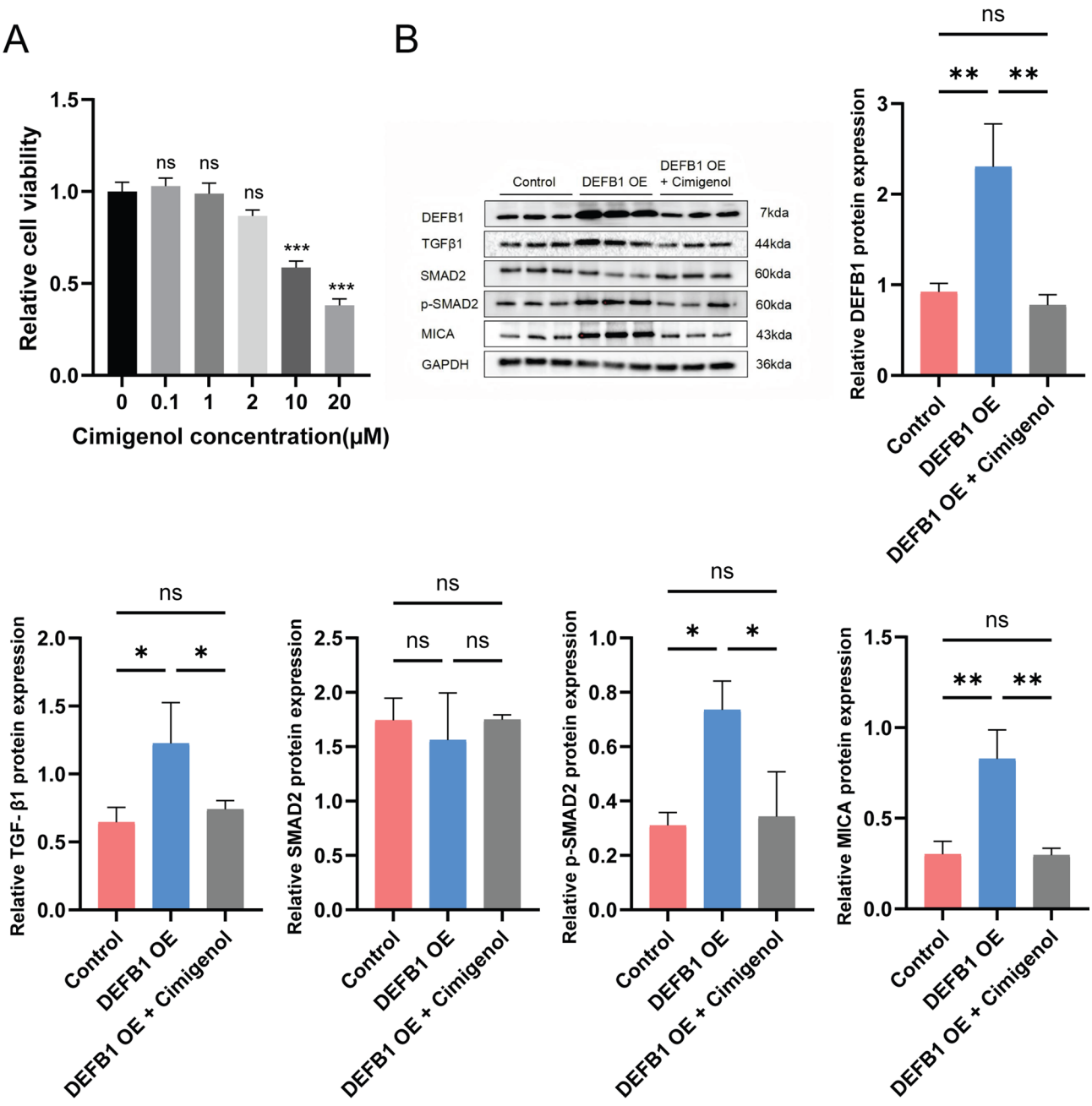

Fig. 8 The Cimigenol treatment inhibited the TGFβ/SMAD2 pathway activation and increased level of MICA induced by DEFB1 in vitro. (**A**) Cell viability of HaCaT cells in different concentrations of Cimigenol. (**B**) The Cimigenol treatment reversed the increase in the protein level of DEFB1, TGFβ1, p-SMAD2, and MICA after the transfection

Currently, there is very limited evidence implicating CYB5D2 in the pathogenesis of AA, which remains to be investigated in the future.

ADGRE2 was identified as a potential protective factor for AA in the deCODE cohort, the causal effect of which was not validated in the UKB cohort. However, a meta-analysis conducted on the results from the two independent cohorts supported its protective effect on AA. Mutation of ADGRE2 was reported to induce dermal degranulation of mast cells and lead to vibratory urticaria [45]. It also contributes to the differentiation and inflammatory activation of human monocytic cells through the NF-κB signaling pathways [46].

The advantage of the current study is that the data resources for both exposure (circulating proteins) and outcome (AA) contained a large sample size and rich coverage of plasma proteins. By employing MR methods, the consistent associations between drug targets from

two independent GWAS datasets and AA confirmed the robustness of the findings. The RNA expression of the identified targets was further analyzed in the GEO dataset GSE212447, which contained lesional samples as the diseased group and healthy samples as the control group, providing new insights into the possible mechanism of the causal relationship between drug targets and AA. Although direct evidence to prove the promoting or inhibiting effects of drug-target proteins on the disease remains unclear, our study still establishes a foundation for the possible use of Cimigenol in AA treatment and provides evidence for further experimental research. Furthermore, the Phe-MR results revealed no side effects, except for an increased risk of sepsis associated with DEFB1. This finding can be viewed positively, given that our study aimed to identify methods to inhibit DEFB1 expression.

However, our study had some limitations. First, data on exposure and outcome were obtained from GWAS in European descendants. Genetic heterogeneity among ethnicities may reduce the potential of prioritized proteins as drug targets in other populations. Second, our study employed the Bonferroni correction and a strict significance threshold for the selection of drug targets, which may increase the risk of ruling out proteins with the potential to be drug targets. The limited number of drug targets increases the difficulty of investigating the related pathways in the pathogenesis of AA. Finally, the expression of some drug targets (e.g., HGFAC) was not detected in almost any type of cell in either scRNA sequence dataset. The connection between local transcriptional expression and circulating proteins needs to be further investigated to clarify their causal effects on AA.

Conclusion

Three circulating proteins, DEFB1, HGFAC, and CYB5D2, were identified as potential drug targets with high value for the treatment of AA. The possible side effects of these drug targets are minor, making it desirable to reuse approved drugs or develop new drugs that target these proteins. The expression of these five drug targets was also altered in different cell types in lesional samples of patients with AA. The TCM ingredient cimigenol was prioritized as a drug that inhibited DEFB1.

Abbreviations

AA	Alopecia areata
ADGRE2	Adhesion G Protein-Coupled Receptor E2
CI	Confidence interval
DEFB1	Beta-defensin 1
GEO	Gene Expression Omnibus
GWAS	Genome-wide association study
HGFAC	Hepatocyte growth factor activator
MICA	MHC class I polypeptide-related sequence A
MM/PBSA	Molecular Mechanics/Poisson-Boltzmann Surface Area
MR	Mendelian randomization
CYB5D2	Cytochrome B5 Domain Containing 2
pQTL	Protein quantitative trait loci
scRNA	Single-cell RNA
SNP	Single nucleotide polymorphism

Supplementary Information

The online version contains supplementary material available at https://doi.org/10.1186/s12014-025-09544-6.

Additional file 1: The 3D plot of the free-energy landscape (FEL) shows the distribution of free energy across different conformations of the system.

Additional file 2: The results of MR analysss as well as the Bonferroni correction and the relevant sensitive analyses performed between three independent cohorts as the exposures and AA as the outcome.

Additional file 3: The potential side effects of three drug target proteins revealed by the Phe-MR.

Acknowledgements

Not applicable.

Author contributions

Lingbo Bi and Jing Wang were responsible for conceptualization, data curation, investigation, and writing the original draft. Jungang Yang contributed their expertise in methodology and software development. Kejun Chen carried out the investigation. Zining Xu and Zhou Zhuang validated and visualized of the results. The resource was acquired by Xianbo Zuo and Jingkai Xu. The project was supervised and funded by Yujun Sheng and Yong Cui, who also reviewed and edited of the manuscript.

Funding

This study was supported by the China National Key R&D Program of China (2022YFC3602002), China-Japan Friendship Hospital Youth Science and Technology Excellence Project (ZRJY2023-GG14), Outstanding Youth Project of Natural Science Foundation of Anhui Province (2208085Y25), National High Level Hospital Clinical Research Funding (2022-NHLHCRF-LX-02-03).

Data availability

All data used in this study is contained in the manuscript, figures, and supplementary materials of this paper.

Declarations

Ethics approval and consent to participate

Not applicable. All data used in this study is publicly available, the ethical approval of which had been obtained by the original researchers from their respective institutional review boards and informed consent from all participants.

Consent for publication

Not applicable.

Competing interests

The authors declare no competing interests.

Received: 5 February 2025 / Accepted: 13 May 2025
Published online: 29 May 2025

References

1. Pratt CH, King LE Jr., Messenger AG, Christiano AM, Sundberg JP. Alopecia areata. Nat Rev Dis Primers. 2017;3:17011. https://doi.org/10.1038/nrdp.2017.11.
2. Rudnicka L, et al. European expert consensus statement on the systemic treatment of alopecia areata. J Eur Acad Dermatol Venereol. 2024;38:687–94. https://doi.org/10.1111/jdv.19768.

3. Trüeb RM, Dias M. Alopecia areata: a comprehensive review of pathogenesis and management. Clin Rev Allergy Immunol. 2018;54:68–87. https://doi.org/10.1007/s12016-017-8620-9.
4. Toussi A, Barton VR, Le ST, Agbai ON, Kiuru M. Psychosocial and psychiatric comorbidities and health-related quality of life in alopecia areata: A systematic review. J Am Acad Dermatol. 2021;85:162–75. https://doi.org/10.1016/j.jaad.2020.06.047.
5. Ramírez-Marín HA, Tosti A. Emerging drugs for the treatment of alopecia areata. Expert Opin Emerg Drugs. 2022;27:379–87. https://doi.org/10.1080/14728214.2022.2149735.
6. Sterkens A, Lambert J, Bervoets A. Alopecia areata: a review on diagnosis, immunological etiopathogenesis and treatment options. Clin Exp Med. 2021;21:215–30. https://doi.org/10.1007/s10238-020-00673-w.
7. Zucchelli F, Harries M, Messenger A, Montgomery K. Establishing the financial burden of alopecia areata and its predictors. Skin Health Dis. 2024;4:e301. https://doi.org/10.1002/ski2.301.
8. Jeon JJ, et al. Global, regional and National epidemiology of alopecia areata: a systematic review and modelling study. Br J Dermatol. 2024;191:325–35. https://doi.org/10.1093/bjd/ljae058.
9. Sawamura S, et al. Elevation of Circulating DNAs of disease-associated cytokines in serum cell-free DNA from patients with alopecia areata. Biosci Trends. 2024;18:198–200. https://doi.org/10.5582/bst.2024.01084.
10. Luo Q, Cao Q, Guo J, Chang S, Wu Y. Genetically predicted levels of Circulating cytokines and the risk of six immune skin diseases: a two-sample Mendelian randomization study. Front Immunol. 2023;14:1240714. https://doi.org/10.3389/fimmu.2023.1240714.
11. Evans DS. Target discovery for drug development using Mendelian randomization. Methods Mol Biol. 2022;2547:1–20. https://doi.org/10.1007/978-1-0716-2573-6_1.
12. Sun BB, et al. Plasma proteomic associations with genetics and health in the UK biobank. Nature. 2023;622:329–38. https://doi.org/10.1038/s41586-023-06592-6.
13. Pietzner M, et al. Mapping the proteo-genomic convergence of human diseases. Science. 2021;374:eabj1541. https://doi.org/10.1126/science.abj1541.
14. Yin KF, et al. Systematic druggable genome-wide Mendelian randomization identifies therapeutic targets for sarcopenia. J Cachexia Sarcopenia Muscle. 2024;15:1324–34. https://doi.org/10.1002/jcsm.13479.
15. Wang Q, et al. Rare variant contribution to human disease in 281,104 UK biobank exomes. Nature. 2021;597:527–32. https://doi.org/10.1038/s41586-021-03855-y.
16. Sun X, et al. Multi-omics Mendelian randomization integrating GWAS, eQTL and pQTL data revealed GSTM4 as a potential drug target for migraine. J Headache Pain. 2024;25:117. https://doi.org/10.1186/s10194-024-01828-w.
17. Lin J, Zhou J, Xu Y. Potential drug targets for multiple sclerosis identified through Mendelian randomization analysis. Brain. 2023;146:3364–72. https://doi.org/10.1093/brain/awad070.
18. Ru J, et al. TCMSP: a database of systems Pharmacology for drug discovery from herbal medicines. J Cheminform. 2014;6:13. https://doi.org/10.1186/1758-2946-6-13.
19. Asilian A, Farmani A, Saber M. Clinical efficacy and safety of low-dose oral Minoxidil versus topical solution in the improvement of androgenetic alopecia: A randomized controlled trial. J Cosmet Dermatol. 2023. https://doi.org/10.1111/jocd.16086.
20. Fu S, Zhou Y, Hu C, Xu Z, Hou J. Network Pharmacology and molecular Docking technology-based predictive study of the active ingredients and potential targets of rhubarb for the treatment of diabetic nephropathy. BMC Complement Med Ther. 2022;22:210. https://doi.org/10.1186/s12906-022-03662-6.
21. Alzolibani AA. Preferential recognition of hydroxyl radical-modified superoxide dismutase by Circulating autoantibodies in patients with alopecia areata. Ann Dermatol. 2014;26:576–83. https://doi.org/10.5021/ad.2014.26.5.576.
22. Guttman-Yassky E, et al. Phase 2a randomized clinical trial of dupilumab (anti-IL-4Rα) for alopecia areata patients. Allergy. 2022;77:897–906. https://doi.org/10.1111/all.15071.
23. Gong Y, et al. Serum level of IL-4 predicts response to topical immunotherapy with Diphenylcyclopropenone in alopecia areata. Exp Dermatol. 2020;29:231–8. https://doi.org/10.1111/exd.13758.
24. Zhao C, Wang I, Lehrer RI. Widespread expression of beta-defensin hBD-1 in human secretory glands and epithelial cells. FEBS Lett. 1996;396:319–22. https://doi.org/10.1016/0014-5793(96)01123-4.
25. Baltzer SA, Brown MH. Antimicrobial peptides: promising alternatives to conventional antibiotics. J Mol Microbiol Biotechnol. 2011;20:228–35. https://doi.org/10.1159/000331009.
26. Farag AGA, et al. Human beta-defensin 1 Circulating level and gene polymorphism in non-segmental vitiligo Egyptian patients. Bras Dermatol. 2023;98:181–8. https://doi.org/10.1016/j.abd.2022.04.002.
27. Calderon C, et al. A multicenter photoprovocation study to identify potential biomarkers by global peptide profiling in cutaneous lupus erythematosus. Lupus. 2015;24:1406–20. https://doi.org/10.1177/0961203315596077.
28. Álvarez Á, Martínez Velázquez H. Prado Montes de Oca, E. Human β-defensin 1 update: potential clinical applications of the restless warrior. Int J Biochem Cell Biol. 2018;104:133–7. https://doi.org/10.1016/j.biocel.2018.09.007.
29. Pita López ML, et al. Cytomegalovirus seropositivity correlates with both human β-defensin 1 and IFN-γ downregulation in women with obesity. Cytokine. 2023;168:156230. https://doi.org/10.1016/j.cyto.2023.156230.
30. Joly S, Organ CC, Johnson GK, McCray PB Jr., Guthmiller JM. Correlation between beta-defensin expression and induction profiles in gingival keratinocytes. Mol Immunol. 2005;42:1073–84. https://doi.org/10.1016/j.molimm.2004.11.001.
31. Xing L, et al. Alopecia areata is driven by cytotoxic T lymphocytes and is reversed by JAK Inhibition. Nat Med. 2014;20:1043–9. https://doi.org/10.1038/nm.3645.
32. Othumpangat S, Noti JD. β-Defensin-1 Regulates Influenza Virus Infection in Human Bronchial Epithelial Cells through the STAT3 Signaling Pathway. *Pathogens* 12. https://doi.org/10.3390/pathogens12010123 (2023).
33. Duits LA, et al. Inhibition of hBD-3, but not hBD-1 and hBD-2, mRNA expression by corticosteroids. Biochem Biophys Res Commun. 2001;280:522–5. https://doi.org/10.1006/bbrc.2000.4157.
34. Strazzulla LC, et al. Alopecia areata: an appraisal of new treatment approaches and overview of current therapies. J Am Acad Dermatol. 2018;78:15–24. https://doi.org/10.1016/j.jaad.2017.04.1142.
35. Suzuki T, et al. Interleukin-15 is a hair follicle immune privilege guardian. J Autoimmun. 2024;145:103217. https://doi.org/10.1016/j.jaut.2024.103217.
36. Peterle L, Sanfilippo S, Borgia F, Cicero N, Gangemi S. Alopecia areata: A review of the role of oxidative stress, possible biomarkers, and potential novel therapeutic approaches. Antioxid (Basel). 2023;12. https://doi.org/10.3390/antiox12010135.
37. Dai X, et al. A novel cycloartane triterpenoid from Cimicifuga induces apoptotic and autophagic cell death in human colon cancer HT-29 cells. Oncol Rep. 2017;37:2079–86. https://doi.org/10.3892/or.2017.5444.
38. Xia HM, Dai YP, Sun LL. [Research progress on cycloartane triterpenoids of Actaea]. Zhongguo Zhong Yao Za Zhi. 2018;43:4000–10. https://doi.org/10.19540/j.cnki.cjcmm.20180703.011.
39. Colin-Pierre C, et al. The Glypican-1/HGF/C-Met and Glypican-1/VEGF/VEGFR2 ternary complexes regulate hair follicle angiogenesis. Front Cell Dev Biol. 2021;9:781172. https://doi.org/10.3389/fcell.2021.781172.
40. Nicu C, et al. Dermal adipose tissue secretes HGF to promote human hair growth and pigmentation. J Invest Dermatol. 2021;141:1633–e16451613. https://doi.org/10.1016/j.jid.2020.12.019.
41. Li Y, et al. Hair-growth promoting effect and anti-inflammatory mechanism of Ginkgo biloba polysaccharides. Carbohydr Polym. 2022;278:118811. https://doi.org/10.1016/j.carbpol.2021.118811.
42. Kimura I, et al. Functions of MAPR (membrane-associated progesterone receptor) family members as heme/steroid-binding proteins. Curr Protein Pept Sci. 2012;13:687–96. https://doi.org/10.2174/138920312804142110.
43. Xie Y, et al. CYB5D2 enhances HeLa cells survival of etoposide-induced cytotoxicity. Biochem Cell Biol. 2011;89:341–50. https://doi.org/10.1139/o11-004.
44. Koster MI. Making an epidermis. Ann N Y Acad Sci. 2009;1170:7–10. https://doi.org/10.1111/j.1749-6632.2009.04363.x.
45. Boyden SE, et al. Vibratory urticaria associated with a missense variant in ADGRE2. N Engl J Med. 2016;374:656–63. https://doi.org/10.1056/NEJMoa1500611.
46. I KY, et al. Activation of adhesion GPCR EMR2/ADGRE2 induces macrophage differentiation and inflammatory responses via Gα(16)/Akt/MAPK/NF-κB signaling pathways. Front Immunol. 2017;8:373. https://doi.org/10.3389/fimmu.2017.00373.

Publisher's note